CELL BIOLOGY

Differential regulation of BAX and BAK apoptotic activity revealed by small molecules

Kaiming Li[1,2], Yu Q. Yap[1,2], Donia M. Moujalled[1,2], Fransisca Sumardy[1,2], Yelena Khakham[1,2], Angela Georgiou[1,2], Michelle Jahja[1,2], Thomas E. Lew[1,2,3], Melanie De Silva[1,2], Meng-Xiao Luo[1,2], Jia-nan Gong[4], Zheng Yuan[1,2], Richard W. Birkinshaw[1,2], Peter E. Czabotar[1,2], Kym Lowes[1,2], David C. S. Huang[1,2], Benjamin T. Kile[5], Andrew H. Wei[1,2,3], Grant Dewson[1,2]*†, Mark F. van Delft[1,2]*†, Guillaume Lessene[1,2,6]*†

Defective apoptosis mediated by B cell lymphoma 2 antagonist/killer (BAK) or B cell lymphoma 2–associated X protein (BAX) underlies various pathologies including autoimmune and degenerative conditions. On mitochondria, voltage-dependent anion channel 2 (VDAC2) interacts with BAK and BAX through a common interface to inhibit BAK or to facilitate BAX apoptotic activity. We identified a small molecule (WEHI-3773) that inhibits interaction between VDAC2 and BAK or BAX revealing contrasting effects on their apoptotic activity. WEHI-3773 inhibits apoptosis mediated by BAX by blocking VDAC2-mediated BAX recruitment to mitochondria. Conversely, WEHI-3773 promotes BAK-mediated apoptosis by limiting inhibitory sequestration by VDAC2. In cells expressing both pro-apoptotic proteins, apoptosis promotion by WEHI-3773 dominates, because activated BAK activates BAX through a feed-forward mechanism. Loss of BAX drives resistance to the BCL-2 inhibitor venetoclax in some leukemias. WEHI-3773 overcomes this resistance by promoting BAK-mediated killing. This work highlights the coordination of BAX and BAK apoptotic activity through interaction with VDAC2 that may be targeted therapeutically.

INTRODUCTION

Intrinsic or mitochondrial apoptosis is mainly governed by protein-protein interactions among B cell lymphoma 2 (BCL-2) proteins (*1*). To execute cell death, effector BCL-2 proteins BCL-2–associated X protein (BAX) or BCL-2 antagonist/killer (BAK) cause mitochondrial outer membrane permeabilization (MOMP), a critical event in the induction of apoptosis (*2*). Impaired mitochondrial apoptosis is a hallmark of cancer (*1*), while excessive cell death is observed under diverse conditions including ischemic brain injury and heart failure (*3*, *4*). Targeting anti-apoptotic BCL-2 proteins to activate apoptosis has transformed the treatment of hematologic malignancies, as evidenced by the incorporation of venetoclax into standard of care for chronic lymphocytic leukemia and acute myeloid leukemia (AML) (*3*). BAK and BAX are proapoptotic effectors essential for the activity of venetoclax and other BCL-2 homology 3 (BH3)–mimetic compounds. Venetoclax inhibits BCL-2 and therefore indirectly unleashes BAK and BAX to initiate apoptosis.

Venetoclax is a highly effective treatment for some blood cancers, but it is rarely curative and most patients relapse after an initial response (*5*, *6*). Thus, acquired tolerance to venetoclax is a growing clinical problem and it is frequently associated with several adaptations that alter the expression or function of BCL-2 family members. Commonly observed changes include mutations to BCL-2 itself (*7*), elevated expression of the prosurvival proteins Myeloid Cell Leukemia 1 (MCL-1) and/or B-Cell Lymphoma-extra large (BCL-XL) (*8*), as well as mutations that impair BAX function (*9*). Hence, there is a need for new drugs to target the apoptosis pathway at multiple levels and more effectively, either to enhance the killing effect of existing treatments like venetoclax or to uncover previously unknown therapeutic vulnerabilities able to tackle the emerging problem of venetoclax resistance. One strategy of interest is to directly modulate the apoptosis effector proteins BAK and/or BAX and enhance their pro-apoptotic activity (*10*–*16*).

Alternatively, excessive apoptosis is observed under diverse conditions including ischemic brain injury, heart failure, and certain degenerative conditions (*3*, *4*). It is unclear whether apoptosis inhibition will be a viable therapeutic strategy under these conditions because of the lack of potent and specific small-molecule inhibitors of BAK and/or BAX to test this hypothesis (*3*).

Directly targeting BAK and BAX to modulate apoptosis has proven challenging, partly due to the complex conformational and localization dynamics of these two proteins and their interactions with lipids within the mitochondrial outer membrane (*2*). Small molecules targeting BAK and BAX to modulate apoptosis have been reported mainly from target-based screening campaigns (*10*–*12*, *16*–*20*), with varying specificity, efficacy, and mechanisms of action (*3*, *14*, *17*–*19*, *21*–*30*).

In addition to BCL-2 family proteins, several non–BCL-2 proteins interact with and regulate BAK and BAX. One well-established example is voltage-dependent anion channel 2 (VDAC2) (*31*), which serves as an adapter to interact with BAK and BAX to regulate their mitochondrial localization and apoptotic activity (*25*, *32*–*36*). We report the discovery of a small molecule that blocks VDAC2 interactions with both BAX and BAK, leading to differential modulation of BAX and BAK apoptotic activity.

[1]Walter and Eliza Hall Institute of Medical Research, Parkville, Victoria, Australia. [2]Department of Medical Biology, University of Melbourne, Parkville, Victoria, Australia. [3]Department of Clinical Haematology, Peter MacCallum Cancer Centre and Royal Melbourne Hospital, Melbourne, Victoria, Australia. [4]National Human Diseases Animal Model Resource Center, National Center of Technology Innovation for Animal Model, Laboratory of Human Disease Comparative Medicine, Institute of Laboratory Animal Sciences, Chinese Academy of Medical Sciences & Peking Union Medical College, Beijing, China. [5]Garvan Institute of Medical Research, Darlinghurst, Sydney, New South Wales, Australia. [6]Department of Biochemistry and Pharmacology, University of Melbourne, Parkville, Victoria, Australia.
*Corresponding author. Email: dewson@wehi.edu.au (G.D.); vandelft@wehi.edu.au (M.F.v.D.); glessene@wehi.edu.au (G.L.)
†These authors contributed equally to this work.

RESULTS

A high-throughput phenotypic screen identifies inhibitors of BAX-driven apoptosis

We undertook a cell-based phenotypic screen to identify inhibitors of BAX-mediated apoptosis. Our previous attempt at developing apoptosis inhibitors in cells expressing both BAX and BAK resulted in inhibitors of BAK-mediated apoptosis (*25*). While these compounds demonstrated potent and on-target activity, they were specific to mouse BAK and thus precluded application in human disease models. To identify inhibitors of BAX with selectivity and cellular potency in human cells, we engineered the human myeloma cell line KMS-12-PE to be dependent on BAX (*BAK*$^{-/-}$) or BAK (*BAX*$^{-/-}$) by CRISPR/Cas9 editing (fig. S1A). *BAK*$^{-/-}$ or *BAX*$^{-/-}$ KMS-12-PE cells remained sensitive to apoptotic cell death induced by the BCL-2 Homology 3 (BH3)-mimetic ABT-737 that inhibits the antiapoptotic proteins BCL-2, BCL-XL, and BCL-W (fig. S1B). Therefore, these cells provided suitable screening platforms to identify compounds able to inhibit either BAX- or BAK-mediated apoptosis.

High-throughput screening of our library comprising 106,572 compounds in *BAK*$^{-/-}$ KMS-12-PE cells, followed by hit validation, led to identification of 17 distinct chemical series able to block BAX-mediated apoptosis induced by an EC_{70} (concentration to induce 70% apoptosis) of ABT-737 assessed by CellTiter-Glo (Fig. 1A). Detailed mechanistic studies concluded that 16 hit series failed to specifically modulate BAX- or BAK-dependent apoptosis (Fig. 1A). In particular, their lack of activity in the mitochondrial depolarization assay suggested that their cell-based activity did not involve directly modulating the apoptotic machinery itself (Fig. 1, B and C) (*37*). Only compound **1** showed activity in both the primary cell viability assay using CellTiter-Glo and the mitochondrial depolarization assay (Fig. 1, B to E). The inhibitory activity was specific to BAX as compound **1** did not inhibit apoptosis in *BAX*$^{-/-}$ or wild-type (WT) KMS-12-PE with functional BAK (fig. S1, C and D).

Intriguingly, the reordered compound **1** sample developed increasing activity over time in our primary cell viability assay. Mass spectrometry indicated several species with molecular weights consistent with oxidation and/or dimerization (fig. S2A). Using a similar substrate analog to screening hit **1**, thiomethyl compound **2**, we were able to reproduce the decomposition profile observed in the screening sample and isolate various components of this mixture (fig. S2B). A high-purity sample of compound **2** exhibited modest BAX inhibitory activity (Supplementary Materials and fig. S2C), whereas the minor fraction corresponding to a molecular weight of 619 (2M-4 of starting compound **2**) exhibited very high potency at blocking ABT-737–induced apoptosis in *BAK*$^{-/-}$ KMS-12-PE cells, with an EC_{50} (median effective concentration) less than 400 nM (Fig. 1, F and G). Using structure determination by two-dimensional nuclear magnetic resonance and other analytical methods, we determine that the active compound corresponded to compound WEHI-3773 (Fig. 1F and Supplementary Materials). We found that a low-yielding, but reliable, method to obtain WEHI-3773 required dry dimethyl sulfoxide (DMSO) and NaI (Supplementary Materials and fig. S2D). All other protocols led to unworkable yields or various other isomers that were inactive in our primary assay.

As initial validation, our screening cascade included orthogonal assays to measure cell viability by propidium iodide (PI) exclusion or mitochondrial depolarization assay on enriched mitochondria (Fig. 1, A and B). Cells were incubated with increasing concentration of WEHI-3773 together with BH3-mimetic compounds at a single EC_{70} concentration, and viability or mitochondrial depolarization was assessed (Fig. 1, A and B). In the viability assay, WEHI-3773 inhibited apoptosis in *BAK*$^{-/-}$ KMS-12-PE cells with an EC_{50} comparable to that measured by CellTiter-Glo (Fig. 1H). In line with its increased cellular potency, WEHI-3773 also exhibited higher activity than compound **1** in the mitochondrial depolarization assay (Fig. 1I). These results confirmed the inhibitory effect of WEHI-3773 on BAX-driven apoptosis observed in the primary screening assay.

WEHI-3773 inhibits BAX mitochondrial targeting and conformation change

Consistent with our observations in KMS-12-PE cells (Fig. 1, H and I), WEHI-3773 also inhibited BAX-driven cell death and mitochondrial depolarization in *BAK*$^{-/-}$ HeLa (fig. S3, A and B, and Fig. 2, A and B), indicating that the BAX inhibitory activity of WEHI-3773 is not restricted to one cell type. The inhibition of mitochondrial depolarization in these two cell lines suggested that WEHI-3773 blocked BAX-driven cell death upstream of MOMP (Fig. 1B). In line with this, WEHI-3773 enabled long-term clonogenic survival of *BAK*$^{-/-}$ HeLa and *BAK*$^{-/-}$ HCT116 cell lines treated with BH3 mimetics ABT-737 and MCL-1 inhibitor S63845, whereas caspase inhibition with quinoline-Val-Asp-difluorophenoxymethylketone (QVD-OPh) did not (Fig. 2, C and D, and fig. S3, C and D).

During apoptosis, BAX undergoes structural changes to adopt an activated conformation that promotes MOMP and cytochrome c release. In doing so, BAX epitopes are exposed, which can be recognized by conformation-specific antibodies (*38*). With these antibody tools, we observed that WEHI-3773 provided dose-dependent inhibition of BAX conformational activation induced by combined BH3 mimetics, and this correlated with a blockade of mitochondrial cytochrome c release (Fig. 2E). Another critical step for BAX to mediate MOMP is its redistribution from the cytosol to mitochondria. Notably, WEHI-3773 also blocked the redistribution of BAX to mitochondria during apoptosis induced by BH3 mimetics, indicating that WEHI-3773 interferes with this key early step in BAX-driven apoptosis (Fig. 2F).

WEHI-3773 prevents VDAC2 from recruiting BAX to mitochondria

A proportion of BAX is associated with mitochondria in healthy cells, even in the absence of an apoptotic stimulus. Notably, culturing cells with WEHI-3773 alone caused BAX to dissociate from mitochondria and be redistributed to the cytosol (Fig. 3A). This phenomenon is reminiscent of the redistribution of BAX in cells lacking VDAC2 (*34*, *36*, *39*) and led us to hypothesize that WEHI-3773 might interfere with the BAX:VDAC2 interaction and, consequently, the recruitment of BAX to mitochondria. Supporting this hypothesis, WEHI-3773 was unable to provoke BAX redistribution from mitochondria that lacked VDAC2 (Fig. 3A and fig. S3E). In addition, WEHI-3773 did not limit BAX-driven cell death in cells lacking VDAC2 (Fig. 3B). To further assess the impact of WEHI-3773 on the BAX:VDAC2 interaction, we performed blue native polyacrylamide gel electrophoresis (BN-PAGE) on mitochondrial fractions isolated from *BAK*$^{-/-}$ HeLa incubated with WEHI-3773. Notably, WEHI-3773 reduced the protein complexes containing BAX and VDAC2 in a dose-dependent manner (Fig. 3C). Together, our data indicate that WEHI-3773 interferes with the BAX:VDAC2 interaction to inhibit BAX targeting to mitochondria (Fig. 3D).

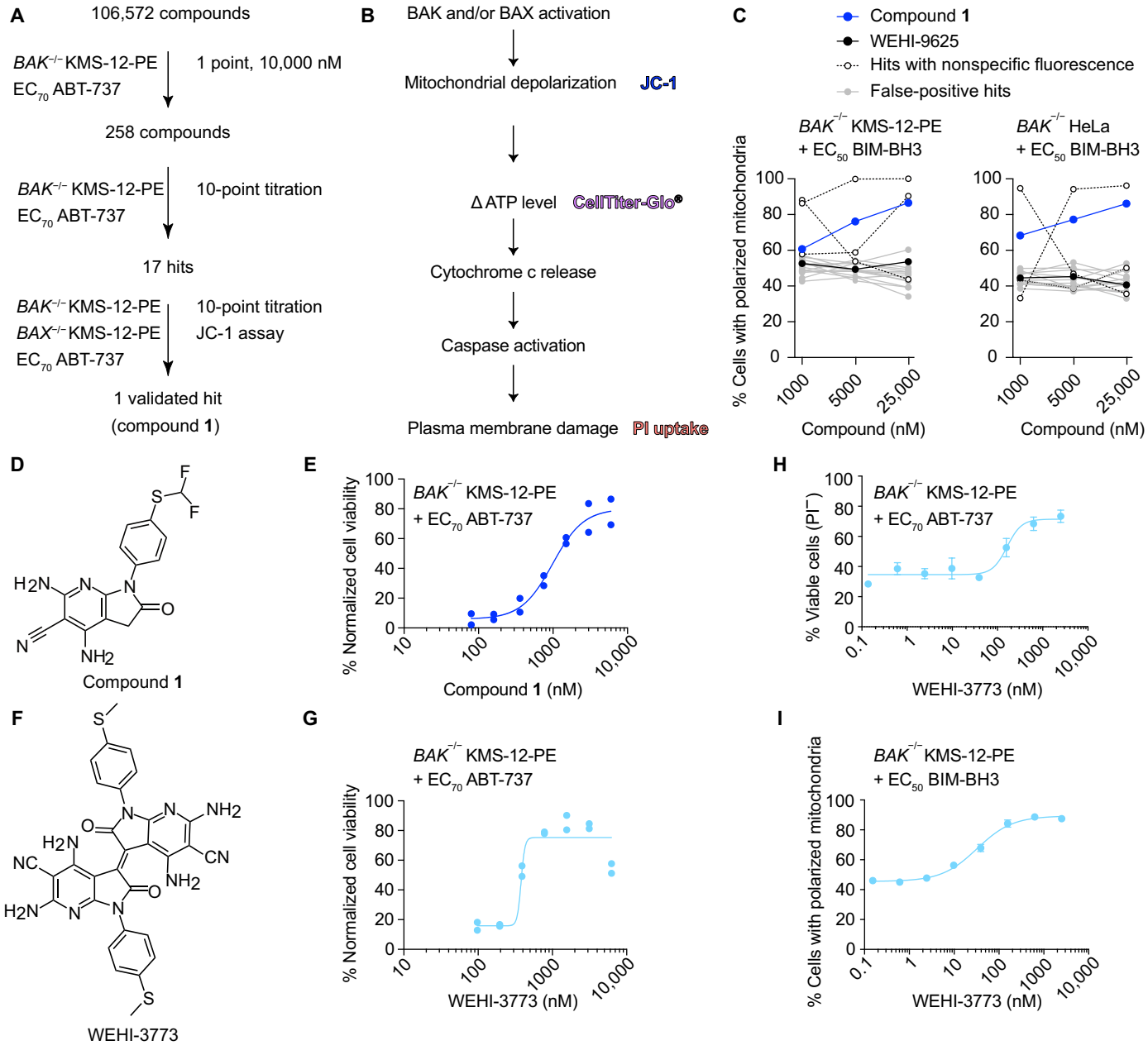

Fig. 1. High-throughput screening identifies inhibitors of BAX-driven apoptosis. (**A**) Experimental workflow and selection criteria used for the discovery of inhibitors of human BAX–driven apoptosis. (**B**) Schematics of assays measuring different steps in the apoptosis pathway. (**C**) Dose-response curves for 17 hit compounds tested on mitochondria in the presence of BIM-BH3 and measured using JC-1 fluorescence assay. WEHI-9625 serves as a control (*25*). Data are from the validation screening cascade, a single experiment. (**D**) Structure of compound 1. (**E**) Dose-response curve for compound 1 tested in the primary screening assay using CellTiter-Glo. Data are from two independent experiments. (**F**) Structure of WEHI-3773. (**G**) Dose-response curve for WEHI-3773 tested in the primary screening assay using CellTiter-Glo. Data are from two independent experiments. (**H**) Dose-response viability curves of KMS-12-PE in the presence of ABT-737, measured by PI uptake and flow cytometry. Data are the means ± SEM of three independent experiments. (**I**) Impact of WEHI-3773 on mitochondrial membrane potential measured by JC-1 staining and flow cytometry in the presence of human BIM-BH3 peptides. Data are the means ± SEM of three independent experiments.

WEHI-3773 primes BAK activation by destabilizing its interaction with VDAC2

VDAC2 interacts with both BAX and BAK, but it regulates the apoptotic function of these proteins in opposing ways (*32*, *34*, *39*). If WEHI-3773 inhibited BAX by interfering with the BAX:VDAC2 interaction, we hypothesized that it might also affect BAK if it similarly interfered with the BAK:VDAC2 interaction. To test this hypothesis, we evaluated the impact of compound **1** and WEHI-3773 on BAK-driven apoptosis. Intriguingly, and consistent with our hypothesis, these compounds potentiated BAK-driven apoptosis in $BAX^{-/-}$ and WT KMS-12-PE and HeLa cells (Fig. 4, A and B, and fig. S1, C and D). Furthermore, WEHI-3773 also potentiated BAK-driven, Bcl-2 Interacting Mediator of cell death (BIM)-induced depolarization of mitochondria in $BAX^{-/-}$ and WT HeLa (Fig. 4C).

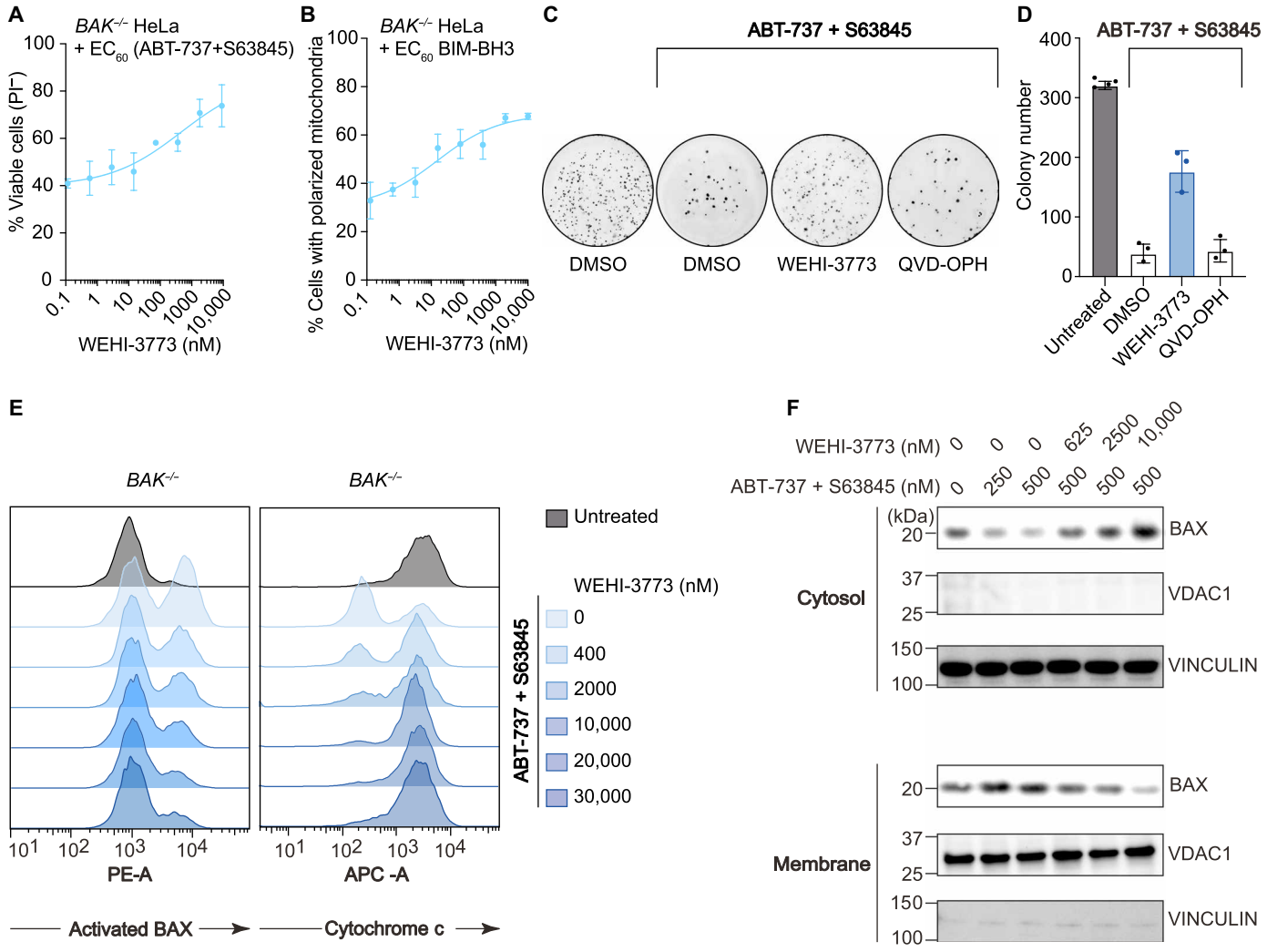

Fig. 2. WEHI-3773 inhibits BAX activation and translocation to limit MOMP and protect cells. (**A**) WEHI-3773's dose-dependent inhibition of cell death in *BAK*$^{-/-}$ HeLa treated with ABT-737 and S63845, measured by PI uptake and flow cytometry. Data are the means ± SEM of three independent experiments. (**B**) WEHI-3773's dose-dependent inhibition of mitochondrial depolarization induced by the BIM-BH3 peptide. Depolarization was measured by JC-1 staining and flow cytometry. Data are the means ± SEM of three independent experiments. (**C**) Representative images of colony formation assay using *BAK*$^{-/-}$ HeLa after 5 days of culture. (**D**) Quantification of colony number. Data are the means and SEM of three independent experiments. (**E**) Intracellular staining and flow cytometry to measure conformationally activated BAX and cytochrome c in *BAK*$^{-/-}$ HeLa. (**F**) Western blot analysis of *BAK*$^{-/-}$ HeLa treated with WEHI-3773, ABT-737, and S63845 at indicated concentrations for 2 hours. Representative blots from $n = 3$ independent experiments are shown. Cytosol and membrane fractions are from the same blot (see the Supplementary Materials) but have been separated for ease of comparison.

We confirmed that WEHI-3773 primed BAK conformational activation, as detected with a conformation-specific antibody, and cytochrome c release in a dose-dependent manner (Fig. 4D). Furthermore, just as WEHI-3773 had the capacity to inhibit BAX in *Vdac2*$^{+/+}$ but not *Vdac2*$^{-/-}$ mouse embryonic fibroblasts (MEFs) (Fig. 3B), it also primed BAK-mediated death in *Vdac2*$^{+/+}$ but not *Vdac2*$^{-/-}$ MEFs (fig. S4A and Fig. 4E). Thus, VDAC2 determines the capacity for WEHI-3773 to influence both BAX and BAK.

Notably, WEHI-3773 in the absence of BH3-mimetic treatment did not induce killing (fig. S4, B and C), suggesting that while it may not induce apoptosis in its own right, WEHI-3773 might synergize with, or potentiate, other sublethal apoptotic signals. Consistent with these observations, WEHI-3773 alone did not dissociate BAK from VDAC2 or activate BAK (fig. S4, D and E), but it did prime BAK dissociation from VDAC2 when combined with low concentrations of BH3 mimetics (Fig. 4F).

To understand whether the differential effect of WEHI-3773 on BAX and BAK was due to their different subcellular localization, we tested the effect of the compound on BAX S184L, a mutant form of BAX that constitutively localizes to mitochondria (*38*). Like BAK, BAX S184L forms a stable complex with VDAC2 in healthy cells and dissociates from VDAC2 when activated (*34*). As with its effect on BAK, but in contrast to its effect on WT BAX, WEHI-3773 potentiated apoptosis in *Bak*$^{-/-}$ *Bax*$^{-/-}$ MEFs engineered to express BAX S184L (Fig. 4G) only when combined with sublethal apoptotic stress signals (fig. S4F). Together, these data indicate that WEHI-3773 inhibits the interactions between VDAC2 and BAK or BAX (Figs. 3D and 4H). The distinct localization and pathway to activation on the

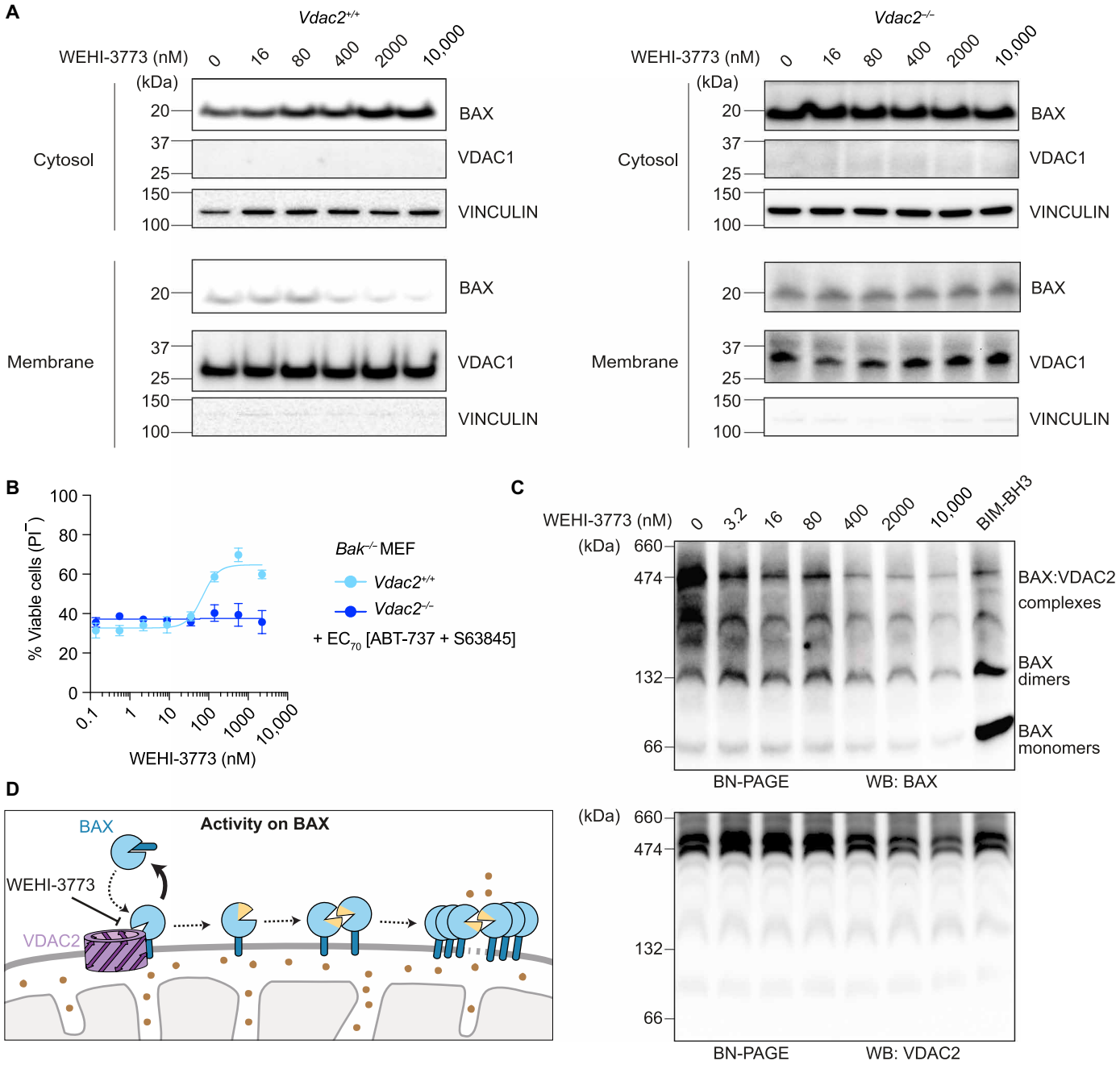

Fig. 3. WEHI-3773 inhibits VDAC2-mediated BAX recruitment to mitochondria. (**A**) Western blot analysis of *Vdac2*$^{-/-}$ or *Vdac2*$^{+/+}$ MEFs treated with WEHI-3773 alone at indicated concentrations for 2 hours. Representative blots of at least three independent experiments are shown. Cytosol and membrane fractions for each genotype are from the same blot (see the Supplementary Materials) but have been separated for ease of comparison. (**B**) Dose-response viability curves of *Bak*$^{-/-}$ MEFs measured by PI uptake and flow cytometry. Cells were pretreated with WEHI-3773 for 2 hours first, and then EC_{70} concentrations of ABT-737 and S63845 were added for another 22 hours before measurement. Data are the means ± SEM of three independent experiments. (**C**) Western blot (WB) analysis of *BAK*$^{-/-}$ mitochondria treated with WEHI-3773 or human BIM-BH3 peptide at indicated concentrations for 30 min, followed by BN-PAGE. Representative blots of at least three independent experiments are shown. (**D**) Proposed working model showing that WEHI-3773 acts on inhibiting BAX:VDAC2 interaction on mitochondria (gray) to limit MOMP and release of mitochondrial factors (brown dots).

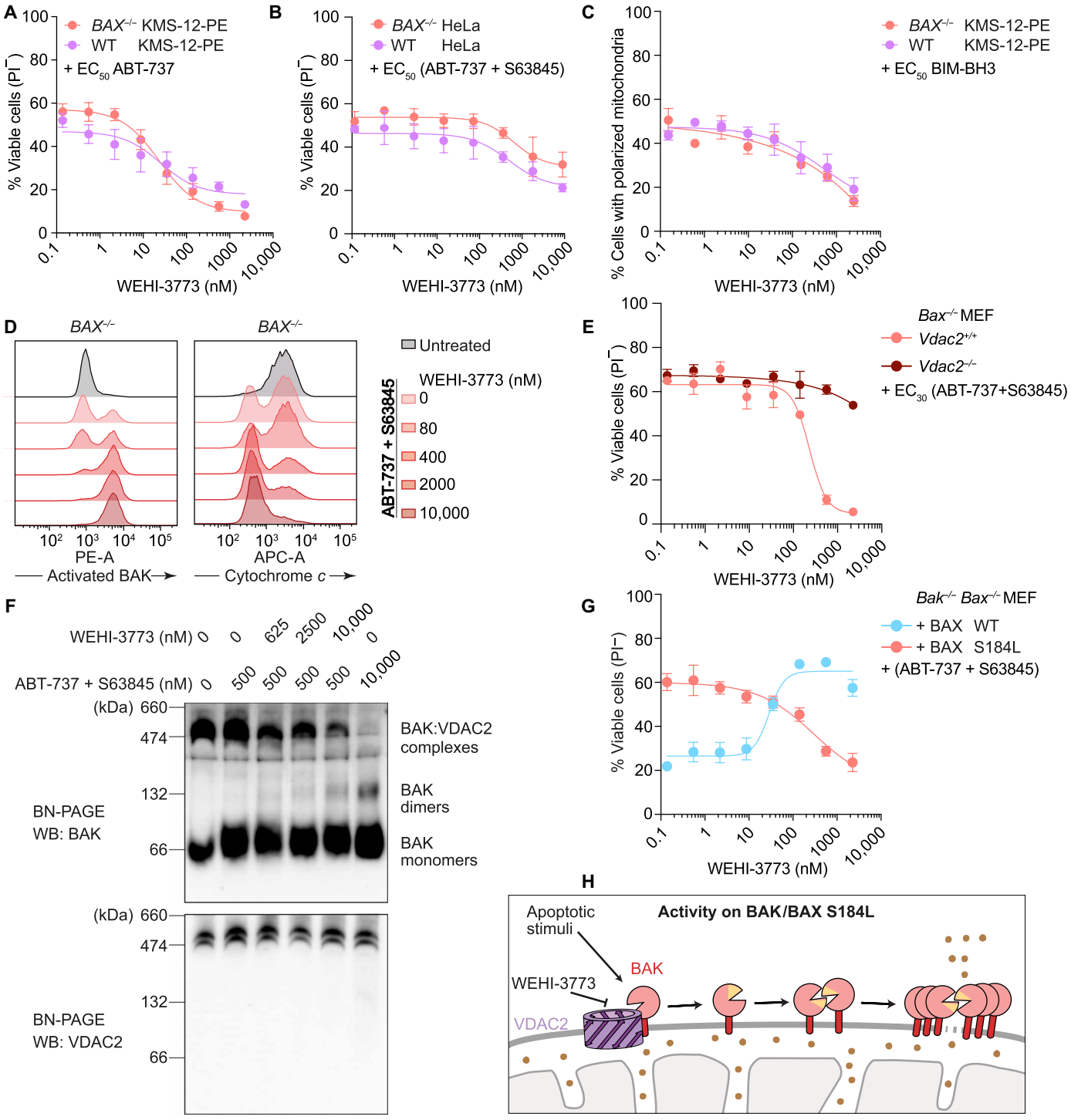

Fig. 4. WEHI-3773 potentiates BAK activation by destabilizing the BAK:VDAC2 interaction. (**A** and **B**) WEHI-3773's potentiation of cell death combined with BH3 mimetics, measured by PI uptake and flow cytometry. Data are the means ± SEM of three independent experiments. (**C**) Impact of WEHI-3773 on mitochondrial membrane potential measured by JC-1 staining and flow cytometry. Means ± SEM of three independent experiments. (**D**) Intracellular staining and flow cytometry to measure activated BAK and preserved cytochrome c level within *BAX*$^{-/-}$ HeLa. (**E**) WEHI-3773's impact on cell death in MEFs, measured by PI uptake and flow cytometry. Cells were pretreated with WEHI-3773 for 2 hours, and then ABT-737 and S63845 (2.4 nM for *Vdac2*$^{-/-}$ *Bax*$^{-/-}$ MEFs and 40 nM for *Vdac2*$^{+/+}$ *Bax*$^{-/-}$ MEFs) were added for another 22 hours. Means ± SEM of three independent experiments. (**F**) BN-PAGE of *BAX*$^{-/-}$ HeLa treated with compounds for 2 hours. Representative blots of three independent experiments are shown. (**G**) Dose response in MEFs re-expressing indicated BAX variants, measured by PI uptake and flow cytometry. Means ± SEM of three independent experiments. (**H**) Schematic model for WEHI-3773 on mitochondria (gray) to potentiate MOMP and release of mitochondrial factors (brown dots).

mitochondrial outer membrane of these two proteins and their propensity to form stable interactions with VDAC2 may underpin the divergence in functional outcomes. In cells expressing both BAK and BAX, BAX conformational activation was promoted rather than inhibited by WEHI-3773 (fig. S4G). This is likely due to the feed-forward amplification of BAX activation by activated BAK on mitochondria, a process that is independent of VDAC2 (fig. S4H) (*40*). Given the fact that WEHI-3773 inhibits BAX in the absence of BAK but promotes BAX activation when BAK is expressed or when BAX is targeted to mitochondria, we reasoned that WEHI-3773 did not interact with BAX or BAK directly to regulate their activity. Given that WEHI-3773 consistently modulated apoptosis provoked by BH3 mimetics in multiple diverse cell lines (Figs. 1, G and H, 2A, 3B, and 4, A, B, E, and G), we tested whether WEHI-3773 could also modulate responses to other apoptotic stimuli. We examined intrinsic [etoposide and staurosporine (STS)] or extrinsic apoptosis stimuli [tumor necrosis factor (TNF) together with cycloheximide (CHX)] using two cell line models: MEFs and HeLa (fig. S5). While the ability of WEHI-3773 to inhibit BAX-mediated apoptosis or to promote BAK-mediated apoptosis was preserved in some cases (e.g., in *Bak*$^{-/-}$ MEF and *BAX*$^{-/-}$ HeLa with STS), in other contexts, these actions were either absent or less pronounced. The limited effects on TNF/CHX–induced killing are possibly due to the death being at least partly BAX/BAK independent, while the variation with STS and etoposide across cellular contexts may reflect the pleiotropic nature of these stimuli and nuances in how they engage the apoptosis machinery.

WEHI-3773 targets VDAC2 to modulate BAK and BAX

Because WEHI-3773 could inhibit both BAK:VDAC2 and BAX:-VDAC2 interactions, we investigated whether WEHI-3773 directly engaged VDAC2 in cells. In our previous work, we discovered a small molecule, WEHI-9625, that interacts with VDAC2 to specifically inhibit mouse BAK (*25*). WEHI-9625 does not affect apoptosis driven by either human BAK or BAX (fig. S6A) (*25*). We have also shown using probes derived from WEHI-9625 that this compound directly interacts with both human and mouse VDAC2 (*25*). We speculated that if WEHI-9625 and WEHI-3773 both interacted with VDAC2, they may do so competitively if their binding sites overlapped or were linked allosterically. If true, then although WEHI-9625 is not capable of influencing human BAK– or BAX-driven apoptosis on its own (fig. S6A), it might interfere with the impact of WEHI-3773 on these proteins. Consistent with this, in KMS-12-PE engineered to lack either BAK or BAX, WEHI-9625 reduced the capacity of WEHI-3773 to both inhibit BAX-driven cell death and prime BAK-driven apoptosis (Fig. 5, A and B). That WEHI-9625 blocks WEHI-3773's activity suggests that, like WEHI-9625, WEHI-3773 also engages VDAC2 in cells.

To confirm the interaction between WEHI-3773 and VDAC2, we performed a drug affinity responsive target stability (DARTS) assay (*41*) on the basis of the assumption that WEHI-3773 binding to VDAC2 would affect VDAC2 stability against proteolysis. Incubation of mitochondria isolated from HCT116 cells with WEHI-3773 inhibited the proteolysis of VDAC2 in a dose-dependent manner, supporting the engagement of VDAC2 by WEHI-3773 on the mitochondrial membrane (Fig. 5, C and D). Consistently, incubation of mitochondria with 400 nM WEHI-3773 inhibited the proteolysis of VDAC2 with increasing concentrations of proteinase K (fig. S6, B and C).

We next sought to determine whether WEHI-3773 directly engages VDAC2 protein and whether the native mitochondrial environment is required for the interaction. To this end, we expressed and purified recombinant full-length human VDAC1 and VDAC2 proteins using *Escherichia coli* (fig. S7, A and B). In line with the observations on mitochondria, WEHI-3773 inhibited the proteolysis of recombinant VDAC2 but not VDAC1 in solution (Fig. 5, E and F). These results suggest that WEHI-3773 directly targets VDAC2 both on mitochondria and in solution.

On the basis of the expression of VDAC1/VDAC2 chimeric proteins, previous studies identified β7 to β10 as the region of VDAC2 interacting with both BAK and BAX (*33*, *39*) (Fig. 5G and fig. S8A). This region on VDAC2 is also necessary for WEHI-9625 to inhibit mouse BAK–driven apoptosis (*25*). To further understand whether this β7-to-β10 region on VDAC2 mediates the action of WEHI-3773, we expressed VDAC1/VDAC2 chimeric proteins in *Bax*$^{-/-}$*Vdac2*$^{-/-}$ MEFs (fig. S8, B and C). Consistent with the competitive relationship between WEHI-9625 and WEHI-3773, substitution of VDAC1 β7 to β10 with the equivalent amino acid sequence from VDAC2 was sufficient to retain the capacity for WEHI-3773 to prime BAK-driven apoptosis (Fig. 5H). Conversely, replacement of that region in VDAC2 with the equivalent amino acid sequence from VDAC1 abolished its activity (Fig. 5H). Together, these results indicate that WEHI-3773 targets VDAC2 protein directly and the region including β7 to β10 on VDAC2 is necessary and sufficient for the activity of WEHI-3773.

WEHI-3773 overcomes venetoclax resistance in leukemic cells

Our previous studies identified loss-of-function BAX mutations as a mechanism of adaptive resistance to venetoclax-based therapy in patients with AML (*9*). Furthermore, we demonstrated that BAX-deficient leukemic cells were largely resistant to BCL-2–targeted compounds administered alone or in combination with other BH3 mimetics (*9*). Thus, we hypothesized that WEHI-3773 could resensitize BAX-deficient human leukemic cells to venetoclax by priming BAK activation. To examine this, we deleted BAX in MV4;11 cells by CRISPR/Cas9 gene editing to render them resistant to venetoclax (Fig. 6, A and B) and tested their responses to various BH3 mimetics combined with WEHI-3773. At 200 nM, WEHI-3773 significantly sensitized these resistant MV4;11 cells to venetoclax (Fig. 6C), supporting our hypothesis that WEHI-3773 can overcome venetoclax resistance upon loss of BAX.

In addition to venetoclax, which has already been approved by the Food and Drug Administration, MCL-1 inhibitors are also being tested in clinical trials for AML (*42*). In our previous study, we also found that loss of BAX, but not its close relative BAK, could confer resistance to MCL-1 inhibitors in AML (*9*). WEHI-3773 could also sensitize resistant MV4;11 cells to the MCL-1 inhibitor S63845 and the combination of venetoclax with S63845 (Fig. 6, D and E), confirming that this compound can resensitize BAX-deficient human leukemic cells to inhibition of different antiapoptotic BCL-2 proteins.

Given the promising effects of WEHI-3773 on BAX-deficient leukemic cells that are resistant to venetoclax, we then tested whether WEHI-3773 could promote apoptosis in a model of acquired resistance to BH3 mimetics (*9*). We have previously shown that OCI-AML3 leukemic cells exposed to prolonged treatment with BH3 mimetics acquired inactivating mutations in BAX that rendered them resistant to the BCL-2 inhibitor (BCL2i R), MCL-1 inhibitor

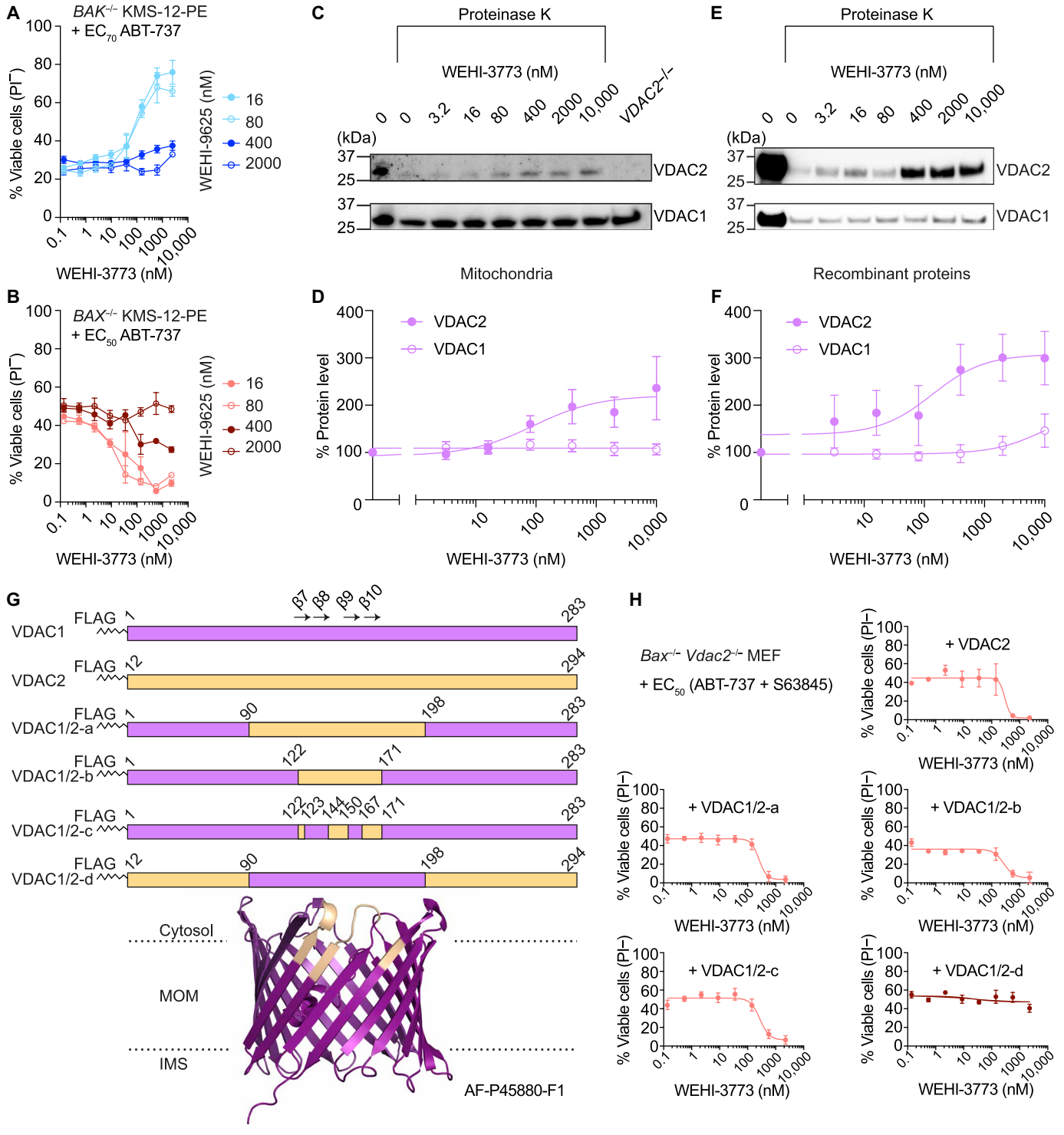

Fig. 5. The β7-to-β10 region of VDAC2 mediates the action of WEHI-3773. (**A** and **B**) Viability of KMS-12-PE cells treated for 48 hours, measured by PI uptake and flow cytometry. Data are the means ± SEM of three independent experiments. (**C**) Immunoblots of mitochondria treated with WEHI-3773 for 30 min, followed by addition of proteinase K. Representative blots of three independent experiments are shown. (**D**) Immunoblots of (C) were quantified and normalized to samples in the second lane. Data are the means ± SEM of three independent experiments. (**E**) Western blot of recombinant proteins treated with WEHI-3773 for 30 min, followed by addition of proteinase K. Representative blots of four independent experiments are shown. (**F**) Immunoblots of (E) were quantified and normalized to samples in the second lane. Data are the means ± SEM of four independent experiments. (**G**) Schematic representation of VDAC1/VDAC2 chimeric constructs and the predicted VDAC2 structure (AF-P45880-F1) (*52*, *53*). VDAC2 is presented as cyan cartoons with the region examined in this study colored gold. IMS, intermembrane space. (**H**) WEHI-3773's impact on cell death in MEFs expressing indicated constructs, measured by PI uptake and flow cytometry. Cells were pretreated with WEHI-3773 for 2 hours, and then ABT-737 and S63845 were added for another 22 hours. Data are the means ± SEM of three independent experiments.

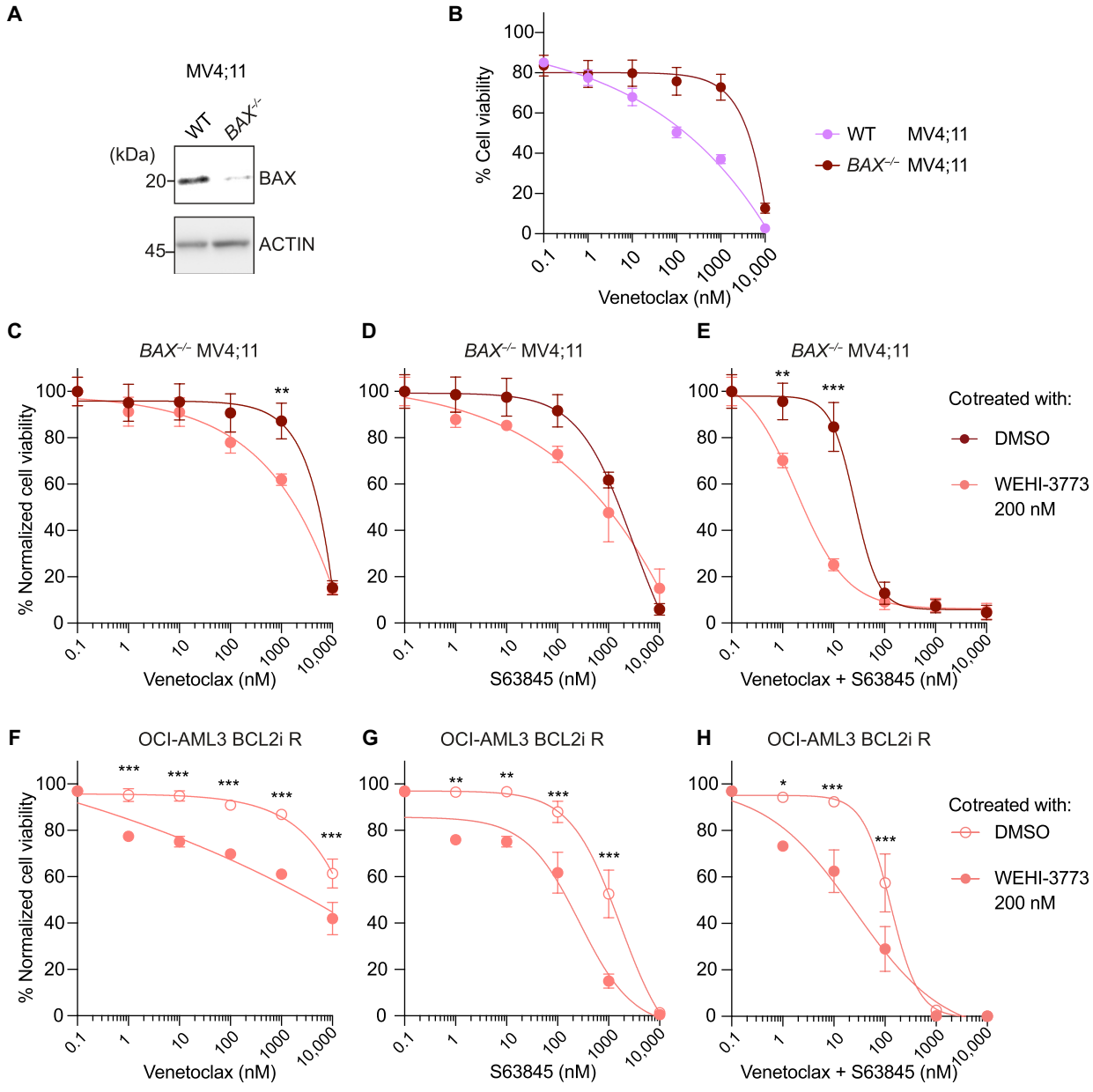

Fig. 6. WEHI-3773 sensitizes BAX-mutant leukemia cells to BH3 mimetics. (**A**) Western blot of lysates from MV4;11 cells transduced with an empty vector or *BAX* guide RNA. (**B**) *BAX*$^{-/-}$ MV4;11 cells were treated with the indicated concentration of BH3 mimetics with or without WEHI-3773 (200 nM) before the assessment of cell viability after 48 hours. (**C** to **E**) *BAX*$^{-/-}$ MV4;11 cells were treated with the indicated concentration of venetoclax (C), S63845 (D), or a combination of venetoclax and S63845 (E) with or without WEHI-3773 before the assessment of cell viability after 48 hours. Data are the means ± SEM of three independent experiments. Two-way analysis of variance (ANOVA) with Tukey test; $^{**}P < 0.01$ and $^{***}P < 0.001$. (**F** to **H**) OCI-AML3 cells rendered resistant to venetoclax (*BCL-2i R*) were treated with the indicated concentration of venetoclax (F), S63845 (G), or a combination of venetoclax and S63845 (H) with or without WEHI-3773 before the assessment of cell viability after 48 hours. Data are means ± SEM of three independent experiments. Two-way ANOVA with Tukey test; $^{*}P < 0.05$, $^{**}P < 0.01$, and $^{***}P < 0.001$.

(MCL1i R), and a combination of both (BCL2i + MCL1i R) (fig. S9A) (*9*). Hence, we tested whether WEHI-3773 could resensitize these resistant OCI-AML3 cells to BH3 mimetics. WEHI-3773 significantly sensitized OCI-AML3 BCL-2i R cells to death induced by venetoclax (Fig. 6F), suggesting that WEHI-3773 could overcome acquired resistance to venetoclax. In addition, WEHI-3773 could also sensitize OCI-AML3 BCL-2i R cells to the MCL-1 inhibitor S63845 (Fig. 6G) or the combination of both (Fig. 6H). These data confirmed that WEHI-3773 can resensitize OCI-AML3 BCL-2i R cells to different BH3 mimetics. Likewise, WEHI-3773 sensitized OCI-AML3 cells that were rendered resistant to MCL-1 inhibition (MCL-1i R) to different BH3 mimetics (fig. S9B). Overall, these data indicate that WEHI-3773 can restore the ability of BH3 mimetics, including venetoclax, to kill leukemic cells with acquired resistance.

The prolonged exposure of OCI-AML3 cells with combined BH3 mimetics (BCL2i + MCL1i) R selects for a loss-of-function BAK

mutant (*9*). Thus, WEHI-3773 did not sensitize (BCL2i + MCL1i) R cells because of the BAK inactivation in these cells (fig. S6C) (*9*). These results indicate that functional BAK capable of driving apoptosis is required for the action of WEHI-3773. In summary, our findings provide a proof of concept that small-molecule enhancement of BAK activity can overcome venetoclax resistance in different leukemic models.

DISCUSSION

Apoptosis mediated by BAK and BAX is aberrant in various human pathologies. Impaired mitochondrial apoptosis is a hallmark of cancer (*1*), while excessive cell death is observed under diverse conditions including ischemic brain injury and heart failure (*3*, *4*). Hence, small molecules that can activate BAK- or BAX-driven apoptosis have the potential to improve treatments for cancer, while blocking these cell death effector proteins might rescue cells from degeneration.

Specific inhibitors of prosurvival BCL-2 proteins have entered the clinic (*43*). In contrast, the development of small molecules that specifically and directly target BAK or BAX to modulate apoptosis has proven more challenging. Several small-molecule inhibitors of BAX and BAK have been reported, including covalent modifiers, that are providing insight into the molecular control of cell death and the tractability of BAX and BAK to treat disease (*17*–*19*, *22*, *28*).

In this study, we used a cell-based phenotypic screen and identified a class of small molecules that differentially modulate both BAX and BAK through their shared interaction with VDAC2. A key feature of phenotypic drug discovery is the opportunity to identify small molecules with novel mechanisms of action. In the case of WEHI-3773, we identified a compound that both inhibits BAX and potentiates BAK-driven apoptosis. Mechanistically, WEHI-3773 targets VDAC2, a channel protein in the mitochondrial outer membrane that interacts with and regulates both BAK and BAX (*31*, *34*, *39*). Notably, its unique mechanism of action reveals the capacity to inhibit BAX only when BAK is expressed at low levels or the proapoptotic function of BAK is restricted. Notably, in certain cell types, such as differentiated neurons, BAK is down-regulated, while BAX expression is maintained; hence, inhibition of BAX alone is sufficient to block apoptosis (*44*). Small molecules acting like WEHI-3773 would be valuable tools to examine the cytoprotective effects of acute BAX inhibition under neurodegenerative conditions.

A clear consequence of disrupting the BAX:VDAC2 interaction with WEHI-3773 is BAX distribution to the cytosol, consistent with *Vdac2* deficiency (*34*, *36*, *39*). This redistribution could be a consequence of enhanced retro-translocation of BAX (*45*, *46*) and aligns with the proposed role of VDAC2 in BAX retro-translocation (*36*). Whether WEHI-3773 promotes active retro-translocation of BAX or whether BAX passively dissociates from mitochondria when its interaction with VDAC2 is destabilized remains unclear.

As shown by the successful development of BH3 mimetics targeting selective prosurvival BCL-2 proteins, activation of apoptosis is a powerful strategy to treat some types of cancers (*47*, *48*). By binding to prosurvival proteins, BH3 mimetics release the brakes on proapoptotic effectors BAK and BAX and thus activate them indirectly. Direct BAK or BAX activators might be another powerful anticancer strategy (*10*–*16*, *20*). However, molecules working in this way might induce broad toxicity. Because WEHI-3773 requires additional apoptotic stimuli to prime but does not alone trigger BAK activity, the toxicity of drugs acting like WEHI-3773 may be manageable. As BAK and BAX are essential for the effective activity of BH3 mimetics, including venetoclax, small molecules that enhance their activity could synergize with BH3 mimetics and potentially overcome resistance to these compounds. By destabilizing the interaction between VDAC2 and BAK, WEHI-3773 is the first molecule to potentiate BAK activation through this mechanism. Hence, we envision that drug-like molecules with a similar mechanism of action to WEHI-3773 could be promising to address the issue of venetoclax resistance by enhancing BAK-dependent apoptosis.

WEHI-3773 alone can disrupt the interaction between BAX and VDAC2. However, it cannot disrupt the interaction between BAK and VDAC2, unless a stimulus is applied to activate BAK. These data suggest that WEHI-3773 shares a binding site with BAX and BAK on VDAC2, but the mechanistic basis for its differential effect on their interactions with VDAC2 remains unclear. We hypothesize that it may relate to the respective conformations of BAX and BAK at the mitochondrial outer membrane. BAX is peripherally associated, whereas BAK is membrane integrated, likely with its C-terminal transmembrane anchor everted. During apoptotic signaling, BAK undergoes a series of conformation changes that promote its dissociation from VDAC2 to allow its homo-oligomerization and pore formation (*32*, *49*, *50*). It is possible that the membrane-integrated conformer of BAK has additional binding sites on VDAC2 that dissociate upon BAK conformation change but cannot be disrupted by WEHI-3773 without apoptotic signaling. While, on its own, WEHI-3773 might not be able to fully dissociate BAK from VDAC2, it is able to destabilize this interface sufficiently to be more sensitive to apoptotic stimuli. Now, structures of BAK (or BAX) in complex with VDAC2 are lacking to provide this insight.

Whereas the apoptosis-modulating effect of WEHI-3773 was evident in multiple diverse cell types when stimulated with BH3 mimetics, its effect on BAX and BAK activity was more variable in response to other types of apoptotic stimuli. Given our evidence that WEHI-3773 modulates BAX and BAK activity at the point of mitochondria, the mechanistic rationale for our observations with the stimuli tested is now unclear but potentially raises intriguing questions around how these more pleiotropic agents engage the apoptosis machinery.

In cells that express both apoptosis effectors, BAX and BAK, the net effect of WEHI-3773 is typically enhanced cell death, as the promotion of BAK activity dominates the inhibitory effect on BAX. Moreover, because activated BAK can induce BAX integration into the mitochondrial outer membrane and conformational activation independently of VDAC2 (*40*), WEHI-3773 effectively promotes both effectors to kill. However, this will likely be context dependent, because in cells with low or functionally impaired BAK, the BAX inhibitory activity of WEHI-3773 may dominate.

Last, our discovery of another VDAC2-targeting compound through a phenotypic drug screen further emphasized the pivotal role of VDAC2 in regulating BAK- and BAX-mediated apoptosis. In line with previous studies (*25*, *34*, *39*), this work shows that the same region on VDAC2 is responsible for engaging BAK and BAX and that this region on VDAC2 can be targeted by small molecules. The fact that WEHI-3773 exhibits a mechanism that is distinct from our previously described mouse BAK inhibitor WEHI-9625 (*25*), while engaging a similar region of VDAC2, suggests that subtle differences in VDAC2 engagement lead to notably different effects on BAX and BAK's ability to drive apoptosis. Moreover, this work demonstrates that although BAK and BAX are challenging targets, modulating

their interaction with VDAC2 can be a successful strategy to affect their apoptotic activity. The structural details of the BAK:VDAC2 and BAX:VDAC2 interfaces remain to be defined (*31*, *33*). This information will inform how to design compounds that selectively influence BAX and BAK apoptotic activity as improved research tools or possibly therapeutics.

MATERIALS AND METHODS

Constructs, antibodies, and reagents

The following constructs were used in this study: FLAG-tagged WT human BAX or FLAG-tagged human BAX S184L was cloned into pMSCV-IRES-GFP. pCMV-VSV-G (Addgene, 8454) and gag/pol (Addgene, 14887) were used for the generation of lentivirus for stable expression.

The following antibodies were used for Western blotting: BAK (no. B5897, Sigma-Aldrich), BAX (no. 49F9, in-house from D. Huang), VDAC2 (no. ab37985, Abcam), VDAC1 (no. ab37985, Millipore), HSP70 (no. MA3-006, Thermo Fisher Scientific), VINCULIN (no. 7000062, Invitrogen), ACTIN (no. sc-47778, Santa Cruz Biotechnologies), TUBULIN (no. 5346S, Cell Signalling Technologies), and FLAG (M2, no. A8592, Sigma-Aldrich). Secondary antibodies anti-rabbit IgG (no. 403005), anti-mouse IgG (no. 103005), anti-rat IgG (no. 303005), and anti-goat IgG (no. 6020-05) were obtained from Southern Biotech.

The following antibodies were used for intracellular staining and flow cytometry. BAK (G317-2, 1:100, no. 556382, BD Pharmingen), BAX (clone 3, 1:100, no. 610982, BD Pharmingen), BAX (clone 6A7, 1:100, BD Pharmingen), cytochrome c-allophycocyanin antibody (no. REA702, 1:50, no. 130111180, Miltenyi Biotec), and phycoerythrin-conjugated anti-mouse antibody (1:200, no. 1031309, Southern Biotech).

The following reagents were used: QVD-OPh (no. OPH109, MP Biomedicals), venetoclax (no. S8048, Selleckchem/Jomar Life Research), ABT-737 (no. A-1002, Active Biochem), A-1331852 (WEHI Chemical Biology Division), S63845 (no. A-6044, Active Biochem), TNF (no. 10602-H01H, Jomar), etoposide (no. 96641, Interpharma), CHX (no. C1988, Sigma-Aldrich), and staurosporine (no. 81590, Cayman).

Cell culture and transient transfection

SV40-transformed MEFs were cultured in Dulbecco's modified Eagle's medium supplemented with 10% (v/v) fetal bovine serum (FBS), 50 μM 2-mercaptoethanol, and 100 μM asparagine. HeLa cells (American Type Culture Collection, no. CCL-2) and human embryonic kidney 293T cells (American Type Culture Collection, no. CRK-3216) were cultured in Dulbecco's modified Eagle's medium supplemented with 10% (v/v) FBS. HCT116 and KMS-12-PE (DSMZ, no. ACC606) cells were cultured in RPMI 1640 supplemented with 10% (v/v) FBS. OCI-AML3 cells were cultured in minimum essential medium α (Gibco) supplemented with 10% (v/v) FBS. MV4;11 cells were cultured in RPMI (Gibco) supplemented with 10% (v/v) FBS. All media contained penicillin (100 IU/ml), streptomycin (100 μg/ml), and L-glutamine (2 mM). Cells were cultured in humidified incubators maintained at 37°C and 10 or 5% CO_2. Cells were routinely screened for mycoplasma contamination using the MycoAlert Kit (cat. no. LT07218, Lonza) as per the manufacturer's instructions. All cell lines were determined to be free of mycoplasma contamination. For transient transfection, constructs were introduced into cells by Lipofectamine 3000 transfection according to the manufacturer's instructions.

Generation of BAX knockout AML cells using CRISPR/Cas9 gene editing

Stable Cas9-expressing human target cells were generated first through lentiviral transduction of target cells with FuCas9Cherry (Addgene plasmid no. 70182), followed by fluorescence-activated cell sorting (FACS) for mCherry expression using a FACSAria (Becton Dickinson: BD). Human stable Cas9 cell lines were subsequently transduced with lentiviral supernatants. Single guide RNAs targeting BAX were synthesized and cloned into FgH1tUTG (Addgene plasmid no. 70183), which permits doxycycline-inducible expression of the single guide RNA and constitutive expression of a green fluorescent protein reporter. All lentiviruses were produced in 293T cells, and cells were transduced using established protocols. The loss of protein expression was confirmed by Western blotting following culture of cells for 72 hours in the presence of doxycycline (5 μg/ml; Sigma-Aldrich, cat. no. 17086-28-1).

Mitochondrial depolarization assay

To assess the mitochondrial membrane potential, the protocol was modified on the basis of a previous publication (*37*). Cells were harvested and washed once with ice-cold phosphate-buffered saline. Cells were resuspended in 300 mM sucrose, 10 mM Hepes-KOH (pH 7.7), 80 mM KCl, 1 mM EDTA, 1 mM EGTA, 5 mM Na succinate, and 0.1% bovine serum albumin with the concentration of 250,000 cells/ ml. Cells were treated with compounds for 10 min at room temperature before the addition of BH3 peptide from human BIM and 0.001% digitonin. After 75-min incubation at room temperature, 5,5′,6,6′-tetrachloro-1,1′,3,3′-tetraethylbenzimidazolylcarbocyanine iodide (JC-1) dye was added to 100 nM. Samples were analyzed using an LSR-II flow cytometer (BD Biosciences).

Colony formation assay

Cells were seeded in a six-well plate at a density of 1000 per well and cultured with indicated concentrations of treatments for 5 days. After treatment, cells were stained with 0.5% crystal violet (cat. no. C0775, Sigma-Aldrich) for 20 min at room temperature and photographed using a ChemiDoc Imaging System (Bio-Rad).

Intracellular staining and flow cytometry

Following indicated treatments, cells were harvested and washed once with ice-cold phosphate-buffered saline. For the assessment of BAK and BAX activation or cytochrome c release, cells were treated with 20 μM caspase inhibitor QVD-OPh for 30 min before treatment with death stimuli. To assess the BAK and BAX conformation change, cell pellets were fixed and then permeabilized using the eBioscience cell fixation and permeabilization kit (cat. no. 88882400, Thermo Fisher Scientific) according to the manufacturer's instructions. Fixed cells were incubated with either a conformation-specific BAK antibody (clone no. G317-2, 1:100, cat. no. 556382, BD Pharmingen) or BAX antibody (clone no. 3, 1:100, cat. no. 610982, BD Pharmingen), followed by a phycoerythrin-conjugated secondary antibody.

To measure cytochrome c release, cells were first permeabilized with 0.025% (w/v) digitonin in permeabilization buffer [20 mM Hepes (pH 7.5), 100 mM sucrose, 2.5 mM $MgCl_2$, and 100 mM KCl] for 10 min on ice before fixation. Fixed cells were incubated with anti-cytochrome c-allophycocyanin antibody (clone no. REA702, 1:50, cat. no. 130111180, Miltenyi Biotec). Samples were analyzed using an LSR-II flow cytometer (BD Biosciences).

Western blotting

Cells were permeabilized with 0.025% (w/v) digitonin for 10 min on ice, and cytosol and heavy membrane fractions were separated by centrifugation at 13,000*g* for 5 min at 4°C. After treatments, membrane fractions were resuspended in lysis buffer [20 mM tris (pH 7.4), 135 mM NaCl, 1.5 mM $MgCl_2$, 1 mM EGTA, and 10% (v/v) glycerol, supplemented with 1% (v/v) digitonin and complete protease inhibitor (0.5 μg/ml; Sigma-Aldrich)] for 30 min on ice. Following lysis, samples were centrifuged at 13,000*g* at 4°C for 10 min and supernatants were collected. Concentrations of cytosolic and heavy membrane proteins were determined using the Bradford protein assay and resolved by SDS-PAGE or BN-PAGE. Gels were transferred onto a polyvinylidene difluoride membrane, and nonspecific binding was blocked with 5% (w/v) nonfat milk in TBS-T [20 mM tris-HCl (pH 7.6), 137 mM NaCl, and 0.1% Tween 20] for 1 hour at room temperature. Membranes were incubated with the primary antibody overnight at 4°C. The membranes were washed three times with TBS-T, followed by incubation with appropriate horseradish peroxidase–conjugated secondary antibodies for 1 hour in room temperature. The membranes were washed with TBS-T (0.01%, v/v) before detection using an enhanced chemiluminescent reagent (Millipore) and imaged using a ChemiDoc Imaging System (Bio-Rad). Protein levels were quantified by densitometric analysis (chemiluminescence) using Image Lab 6.1 software.

High-throughput screening

Assay-ready plates containing compound or controls were prepared. Compounds were screened at a final concentration of 10 μM, and all wells were backfilled with DMSO to final 0.5%. For the high-throughput screening, $BAK^{-/-}$ KMS-12-PE cells were resuspended in RPMI supplemented with 2.5% FBS and seeded into 384-well white tissue culture plates (Greiner, cat. no. 781098) at 20,000 cells per well at 50 μl using a Multidrop Combi reagent dispenser (Thermo Fisher Scientific). The plates were incubated for 2 hours (37°C and 5% CO_2) before addition of 100 nl of ABT-737 (final concentration of 250 nM, previously determined to reduce the viability of $BAK^{-/-}$ KMS-12-PE under these assay conditions to ~30%) by pin-tool transfer. Plates were incubated at 37°C and 5% CO_2 for a further 22 hours, and then CellTiter-Glo (Promega) was added to all wells to determine viability. Luminescence was read on an Envision plate reader (PerkinElmer). Data were archived and analyzed in ActivityBase XE (IDBS), and the TIBCO Spotfire Screening data quality was monitored by Z' for each assay plate. Plates were excluded from analysis if $Z' < 0.5$, and the plates included had an average Z' of 0.65. Data were normalized to percent viability relative to DMSO (100% viability) and EC_{70} ABT-737 (0% viability). Hits were selected on the criteria of % activity >3SD mean of samples in the same experiment.

Generation of stable cell lines

Human embryonic kidney 293T cells were used as virus-packaging cells. The viral constructs were first introduced into packaging cells by Lipofectamine 3000 transfection according to the manufacturer's instructions. Viral supernatants were filtered and used to infect cells by spin-infection (2500-rpm centrifugation at 25°C for 1 hour) in the presence of polybrene (4 μg/ml; cat. no. S2667, Sigma-Aldrich). Transduced cells were enriched by either antibiotic selection or expression of fluorescent protein using a BD FACSAria Fusion cell sorter.

Cell viability assay

Cells were treated as indicated. After treatments, cells were harvested and resuspended in FACS buffer (150 mM NaCl, 3.7 mM KCl, 2.5 M $CaCl_2$, 1.2 mM $MgSO_4$, and 14.8 mM Hepes) with PI (2.5 to 5 μg/ml; Sigma-Aldrich). Cell viability (PI-negative) was assessed using an LSR-II flow cytometer (BD Biosciences).

For cell viability assay with AML cells, cell lines were plated at 2.5×10^5 cells/ml (25,000 cells per well) and treated with six-point 10-fold serial dilution of compounds starting from 10 μM. Cell viability was determined after 48 hours of treatment by FACS analysis of cellular exclusion of SYTOX Blue Dead Cell Stain (Life Technologies, cat. no. S34857) using an LSR-Fortessa (BD). All FACS data were analyzed using FlowJo software.

Recombinant protein expression and purification

Protocols for expression and purification of full-length human VDAC1 (UniProt: P21796) and VDAC2 (UniProt: P45880) were adapted from a previous publication (*51*). Constructs with N-terminally His-tagged VDAC1 and VDAC2 were transformed into BL21 (DE3) and plated with ampicillin (100 μg/ml) overnight at 37°C. Single colonies were picked and inoculated into Luria Broth medium with ampicillin (100 μg/ml) overnight at 37°C with agitation. Overnight starter culture (15 ml) was inoculated into Super Broth medium with ampicillin (100 μg/ml) at 37°C until the optical density at 600 nm reached 1. Protein expression was induced with 1 mM isopropyl β-D-1-thiogalactopyranoside. After another 3 hours of culture, cells were harvested by centrifugation at 4500 rpm for 15 min and frozen at −80°C for further experiments.

The bacterial cell pellet was lysed in lysis buffer [lysozyme, deoxyribonuclease I, 1% Triton X-100, 4 mM $MgCl_2$, and 10 mM dithiothreitol (DTT)] at room temperature for 20 min. Inclusion bodies were prepared after centrifugation at 10,000*g* for 15 min at 4°C and washed three times with wash buffer I [50 mM tris (pH 8.0), 100 mM NaCl, 1 mM EDTA, 1 mM DTT, 0.5% Triton X-100, and protease inhibitors] and one time with wash buffer II [50 mM tris (pH 8.0), 1 mM EDTA, 1 mM DTT, and protease inhibitors] in a Dounce homogenizer. Inclusion bodies were solubilized in 20 mM tris (pH 8.0), 6 M guanidinium, 0.5 mM EDTA, and 1 mM DTT overnight at 4°C. The insoluble pellet was removed by centrifugation at 20,000*g* for 30 min at 4°C. Denatured proteins in supernatants were collected and frozen at −80°C for further experiments.

Refolding of VDAC proteins was performed by dropwise dilution into refolding buffer [20 mM tris (pH 8.0), 300 mM NaCl, 2% *N*,*N*-dimethyldodecylamine *N*-oxide (LDAO), and 1 mM tris(2-carboxyethyl)phosphine (TCEP)] with stirring at 4°C. Protein aggregates were removed by centrifugation at 3500*g* for 20 min at 4°C.

The Ni-NTA column was used for immobilized metal ion affinity chromatography. Proteins were loaded onto the Ni-NTA column followed by washes with more than 10 column volumes of 20 mM tris (pH 8.0), 300 mM NaCl, 0.1% LDAO, and 1 mM TCEP at 4°C. Proteins were eluted with 20 mM tris (pH 8.0), 300 mM NaCl, 0.1% LDAO, 1 mM TCEP, and 250 mM imidazole, pooled, and concentrated.

Proteins were loaded onto a Superdex 200 Increase 10/300 GL size exclusion column (Cytiva) for further purification at 4°C. The column was pre-equilibrated with 20 mM tris (pH 8.0), 300 mM NaCl, 0.1% LDAO, and 1 mM TCEP. After sample loading, proteins were eluted in the same buffer, and fractions were assessed by SDS-PAGE. Fractions with purified proteins were pooled, concentrated, and stored at −80°C.

DARTS assay

Protocols for DARTS assay were adapted from a previous publication (*41*). To perform DARTS assay on mitochondria, cells were first permeabilized with 0.025% (w/v) digitonin in permeabilization buffer [20 mM Hepes (pH 7.5), 100 mM sucrose, 2.5 mM $MgCl_2$, and 100 mM KCl] for 10 min on ice. Membrane fractions were collected after centrifugation at 13,000*g* for 5 min at 4°C. Membrane fractions containing mitochondria were resuspended in permeabilization buffer without digitonin and incubated with compounds or DMSO at 30°C for 30 min. Proteinase K was added in the sample, followed by incubation at 37°C for 30 min. LDS loading dye (Invitrogen) with proteinase inhibitors was added to stop the reaction. Samples were heated at 95°C for 8 min before being loaded for SDS-PAGE followed by Western blotting.

A similar assay was performed on recombinant proteins. Purified proteins were retrieved from −80°C and thawed on ice. Proteins were incubated with compounds or DMSO in 20 mM tris (pH 8.0), 300 mM NaCl, 0.1% LDAO, and 1 mM TCEP at 30°C for 30 min. Proteinase K was added, followed by incubation at 37°C for 30 min. LDS loading dye with proteinase inhibitors was added to stop the reaction. Samples were heated at 95°C for 8 min before being loaded for SDS-PAGE followed by Western blotting.

Statistical analysis

GraphPad Prism 9 was used to perform statistical analyses. All experiments were performed at least three times independently, unless specified. Data are presented as the means ± SEM or SD, as indicated in the figure legends.

Supplementary Materials

This PDF file includes:

Supplementary Text
Figs. S1 to S9
Uncropped blots
References

REFERENCES AND NOTES

1. R. Singh, A. Letai, K. Sarosiek, Regulation of apoptosis in health and disease: The balancing act of BCL-2 family proteins. *Nat. Rev. Mol. Cell Biol.* **20**, 175–193 (2019).
2. T. Moldoveanu, P. E. Czabotar, BAX, BAK, and BOK: A coming of age for the BCL-2 family effector proteins. *Cold Spring Harb. Perspect. Biol.* **12**, a036319 (2020).
3. K. Li, M. F. van Delft, G. Dewson, Too much death can kill you: Inhibiting intrinsic apoptosis to treat disease. *EMBO J.* **40**, e107341 (2021).
4. I. Lei, W. Huang, P. E. Noly, S. Naik, M. Ghali, L. Liu, F. D. Pagani, A. Abou El Ela, J. S. Pober, B. Pitt, J. L. Platt, M. Cascalho, Z. Wang, Y. E. Chen, R. M. Mortensen, P. C. Tang, Metabolic reprogramming by immune-responsive gene 1 up-regulation improves donor heart preservation and function. *Sci. Transl. Med.* **15**, eade3782 (2023).
5. M. A. Anderson, C. Tam, T. E. Lew, S. Juneja, M. Juneja, D. Westerman, M. Wall, S. Lade, A. Gorelik, D. C. S. Huang, J. F. Seymour, A. W. Roberts, Clinicopathological features and outcomes of progression of CLL on the BCL2 inhibitor venetoclax. *Blood* **129**, 3362–3370 (2017).
6. A. W. Roberts, S. Ma, T. J. Kipps, S. E. Coutre, M. S. Davids, B. Eichhorst, M. Hallek, J. C. Byrd, K. Humphrey, L. Zhou, B. Chyla, J. Nielsen, J. Potluri, S. Y. Kim, M. Verdugo, S. Stilgenbauer, W. G. Wierda, J. F. Seymour, Efficacy of venetoclax in relapsed chronic lymphocytic leukemia is influenced by disease and response variables. *Blood* **134**, 111–122 (2019).
7. P. Blombery, M. A. Anderson, J. N. Gong, R. Thijssen, R. W. Birkinshaw, E. R. Thompson, C. E. Teh, T. Nguyen, Z. Xu, C. Flensburg, T. E. Lew, I. J. Majewski, D. H. D. Gray, D. A. Westerman, C. S. Tam, J. F. Seymour, P. E. Czabotar, D. C. S. Huang, A. W. Roberts, Acquisition of the recurrent Gly101Val mutation in BCL2 confers resistance to venetoclax in patients with progressive chronic lymphocytic leukemia. *Cancer Discov.* **9**, 342–353 (2019).
8. R. Thijssen, L. Tian, M. A. Anderson, C. Flensburg, A. Jarratt, A. L. Garnham, J. S. Jabbari, H. Peng, T. E. Lew, C. E. Teh, Q. Gouil, A. Georgiou, T. Tan, T. M. Djajawi, C. S. Tam, J. F. Seymour, P. Blombery, D. H. D. Gray, I. J. Majewski, M. E. Ritchie, A. W. Roberts, D. C. S. Huang, Single-cell multiomics reveal the scale of multilayered adaptations enabling CLL relapse during venetoclax therapy. *Blood* **140**, 2127–2141 (2022).
9. D. M. Moujalled, F. C. Brown, C. C. Chua, M. A. Dengler, G. Pomilio, N. S. Anstee, V. Litalien, E. Thompson, T. Morley, S. MacRaild, I. S. Tiong, R. Morris, K. Dun, A. Zordan, J. Shah, S. Banquet, E. Halilovic, E. Morris, M. J. Herold, G. Lessene, J. M. Adams, D. C. S. Huang, A. W. Roberts, P. Blombery, A. H. Wei, Acquired mutations in BAX confer resistance to BH3-mimetic therapy in acute myeloid leukemia. *Blood* **141**, 634–644 (2023).
10. J. R. Pritz, F. Wachter, S. Lee, J. Luccarelli, T. E. Wales, D. T. Cohen, P. Coote, G. J. Heffron, J. R. Engen, W. Massefski, L. D. Walensky, Allosteric sensitization of proapoptotic BAX. *Nat. Chem. Biol.* **13**, 961–967 (2017).
11. D. E. Reyna, T. P. Garner, A. Lopez, F. Kopp, G. S. Choudhary, A. Sridharan, S. R. Narayanagari, K. Mitchell, B. Dong, B. A. Bartholdy, L. D. Walensky, A. Verma, U. Steidl, E. Gavathiotis, Direct activation of BAX by BTSA1 overcomes apoptosis resistance in acute myeloid leukemia. *Cancer Cell* **32**, 490–505.e10 (2017).
12. G. Sekar, G. Singh, X. Qin, C. D. Guibao, B. Schwam, Z. Inde, C. R. Grace, W. Zhang, P. J. Slavish, W. Lin, T. Chen, R. E. Lee, Z. Rankovic, K. Sarosiek, T. Moldoveanu, Small molecule SJ572946 activates BAK to initiate apoptosis. *iScience* **25**, 105064 (2022).
13. N. Gitego, B. Agianian, O. W. Mak, V. Kumar Mv, E. H. Cheng, E. Gavathiotis, Chemical modulation of cytosolic BAX homodimer potentiates BAX activation and apoptosis. *Nat. Commun.* **14**, 8381 (2023).
14. M. Chen, L. Hu, X. Bao, K. Ye, Y. Li, Z. Zhang, S. H. Kaufmann, J. Xiao, H. Dai, Eltrombopag directly activates BAK and induces apoptosis. *Cell Death Dis.* **14**, 394 (2023).
15. A. Lopez, D. E. Reyna, N. Gitego, F. Kopp, H. Zhou, M. A. Miranda-Roman, L. U. Nordstrom, S. R. Narayanagari, P. Chi, E. Vilar, A. Tsirigos, E. Gavathiotis, Co-targeting of BAX and BCL-XL proteins broadly overcomes resistance to apoptosis in cancer. *Nat. Commun.* **13**, 1199 (2022).
16. D. Park, A. S. M. Anisuzzaman, A. T. Magis, G. Chen, M. Xie, G. Zhang, M. Behera, G. L. Sica, S. S. Ramalingam, T. K. Owonikoko, X. Deng, Discovery of small molecule Bak activator for lung cancer therapy. *Theranostics* **11**, 8500–8516 (2021).
17. A. Z. Spitz, E. Zacharioudakis, D. E. Reyna, T. P. Garner, E. Gavathiotis, Eltrombopag directly inhibits BAX and prevents cell death. *Nat. Commun.* **12**, 1134 (2021).
18. T. P. Garner, D. Amgalan, D. E. Reyna, S. Li, R. N. Kitsis, E. Gavathiotis, Small-molecule allosteric inhibitors of BAX. *Nat. Chem. Biol.* **15**, 322–330 (2019).
19. X. Niu, H. Brahmbhatt, P. Mergenthaler, Z. Zhang, J. Sang, M. Daude, F. G. R. Ehlert, W. E. Diederich, E. Wong, W. Zhu, J. Pogmore, J. P. Nandy, M. Satyanarayana, R. K. Jimmidi, P. Arya, B. Leber, J. Lin, C. Culmsee, J. Yi, D. W. Andrews, A small-molecule inhibitor of Bax and Bak oligomerization prevents genotoxic cell death and promotes neuroprotection. *Cell Chem. Biol.* **24**, 493–506.e5 (2017).
20. H. Brahmbhatt, D. Uehling, R. Al-Awar, B. Leber, D. Andrews, Small molecules reveal an alternative mechanism of Bax activation. *Biochem. J.* **473**, 1073–1083 (2016).
21. M. Matsuyama, J. T. Ortega, Y. Fedorov, J. Scott-McKean, J. Muller-Greven, M. Buck, D. Adams, B. Jastrzebska, W. Greenlee, S. Matsuyama, Development of novel cytoprotective small compounds inhibiting mitochondria-dependent cell death. *iScience* **26**, 107916 (2023).
22. M. W. McHenry, P. Shi, C. M. Camara, D. T. Cohen, T. J. Rettenmaier, U. Adhikary, M. A. Gygi, K. Yang, S. P. Gygi, T. E. Wales, J. R. Engen, J. A. Wells, L. D. Walensky, Covalent inhibition of pro-apoptotic BAX. *Nat. Chem. Biol.* **20**, 1022–1032 (2024).
23. A. Z. Spitz, E. Gavathiotis, Physiological and pharmacological modulation of BAX. *Trends Pharmacol. Sci.* **43**, 206–220 (2022).
24. L. D. Walensky, Targeting BAX to drug death directly. *Nat. Chem. Biol.* **15**, 657–665 (2019).
25. M. F. van Delft, S. Chappaz, Y. Khakham, C. T. Bui, M. A. Debrincat, K. N. Lowes, J. M. Brouwer, C. Grohmann, P. P. Sharp, L. F. Dagley, L. Li, K. McArthur, M. X. Luo, H. S. Chin, W. D. Fairlie, E. F. Lee, D. Segal, S. Duflocq, R. Lessene, S. Bernard, L. Peilleron, T. Nguyen, C. Miles, S. S. Wan, R. M. Lane, A. Wardak, K. Lackovic, P. M. Colman, J. J. Sandow, A. I. Webb, P. E. Czabotar, G. Dewson, K. G. Watson, D. C. S. Huang, G. Lessene, B. T. Kile, A small molecule interacts with VDAC2 to block mouse BAK-driven apoptosis. *Nat. Chem. Biol.* **15**, 1057–1066 (2019).
26. J. Lin, Tightening a deadly pore former. *Nat. Chem. Biol.* **15**, 316–317 (2019).
27. S.-S. Song, W.-K. Lee, S. Aluvila, K. J. Oh, Y. G. Yu, Identification of inhibitors against BAK pore formation using an improved in vitro assay system. *Bull. Korean Chem. Soc.* **35**, 419–424 (2014).
28. P. M. Peixoto, S. Y. Ryu, A. Bombrun, B. Antonsson, K. W. Kinnally, MAC inhibitors suppress mitochondrial apoptosis. *Biochem. J.* **423**, 381–387 (2009).
29. C. Hetz, P. A. Vitte, A. Bombrun, T. K. Rostovtseva, S. Montessuit, A. Hiver, M. K. Schwarz, D. J. Church, S. J. Korsmeyer, J. C. Martinou, B. Antonsson, Bax channel inhibitors prevent mitochondrion-mediated apoptosis and protect neurons in a model of global brain ischemia. *J. Biol. Chem.* **280**, 42960–42970 (2005).
30. A. Bombrun, P. Gerber, G. Casi, O. Terradillos, B. Antonsson, S. Halazy, 3,6-Dibromocarbazole piperazine derivatives of 2-propanol as first inhibitors of cytochrome c release via Bax channel modulation. *J. Med. Chem.* **46**, 4365–4368 (2003).

31. Z. Yuan, G. Dewson, P. E. Czabotar, R. W. Birkinshaw, VDAC2 and the BCL-2 family of proteins. *Biochem. Soc. Trans.* **49**, 2787–2795 (2021).
32. E. H. Cheng, T. V. Sheiko, J. K. Fisher, W. J. Craigen, S. J. Korsmeyer, VDAC2 inhibits BAK activation and mitochondrial apoptosis. *Science* **301**, 513–517 (2003).
33. S. Naghdi, P. Várnai, G. Hajnóczky, Motifs of VDAC2 required for mitochondrial Bak import and tBid-induced apoptosis. *Proc. Natl. Acad. Sci. U.S.A.* **112**, E5590–E5599 (2015).
34. S. B. Ma, T. N. Nguyen, I. Tan, R. Ninnis, S. Iyer, D. A. Stroud, M. Menard, R. M. Kluck, M. T. Ryan, G. Dewson, Bax targets mitochondria by distinct mechanisms before or during apoptotic cell death: A requirement for VDAC2 or Bak for efficient Bax apoptotic function. *Cell Death Differ.* **21**, 1925–1935 (2014).
35. Z. Yuan, M. F. van Delft, M. X. Li, F. Sumardy, B. J. Smith, D. C. S. Huang, G. Lessene, Y. Khakam, R. Jin, S. He, N. A. Smith, R. W. Birkinshaw, P. E. Czabotar, G. Dewson, Key residues in the VDAC2-BAK complex can be targeted to modulate apoptosis. *PLOS Biol.* **22**, e3002617 (2024).
36. J. Lauterwasser, F. Todt, R. M. Zerbes, T. N. Nguyen, W. Craigen, M. Lazarou, M. van der Laan, F. Edlich, The porin VDAC2 is the mitochondrial platform for Bax retrotranslocation. *Sci. Rep.* **6**, 32994 (2016).
37. J. Ryan, A. Letai, BH3 profiling in whole cells by fluorimeter or FACS. *Methods* **61**, 156–164 (2013).
38. A. Nechushtan, C. L. Smith, Y. T. Hsu, R. J. Youle, Conformation of the Bax C-terminus regulates subcellular location and cell death. *EMBO J.* **18**, 2330–2341 (1999).
39. H. S. Chin, M. X. Li, I. K. L. Tan, R. L. Ninnis, B. Reljic, K. Scicluna, L. F. Dagley, J. J. Sandow, G. L. Kelly, A. L. Samson, S. Chappaz, S. L. Khaw, C. Chang, A. Morokoff, K. Brinkmann, A. Webb, C. Hockings, C. M. Hall, A. J. Kueh, M. T. Ryan, R. M. Kluck, P. Bouillet, M. J. Herold, D. H. D. Gray, D. C. S. Huang, M. F. van Delft, G. Dewson, VDAC2 enables BAX to mediate apoptosis and limit tumor development. *Nat. Commun.* **9**, 4976 (2018).
40. S. Iyer, R. T. Uren, M. A. Dengler, M. X. Shi, E. Uno, J. M. Adams, G. Dewson, R. M. Kluck, Robust autoactivation for apoptosis by BAK but not BAX highlights BAK as an important therapeutic target. *Cell Death Dis.* **11**, 268 (2020).
41. B. Lomenick, R. Hao, N. Jonai, R. M. Chin, M. Aghajan, S. Warburton, J. Wang, R. P. Wu, F. Gomez, J. A. Loo, J. A. Wohlschlegel, T. M. Vondriska, J. Pelletier, H. R. Herschman, J. Clardy, C. F. Clarke, J. Huang, Target identification using drug affinity responsive target stability (DARTS). *Proc. Natl. Acad. Sci. U.S.A.* **106**, 21984–21989 (2009).
42. S. T. Diepstraten, M. A. Anderson, P. E. Czabotar, G. Lessene, A. Strasser, G. L. Kelly, The manipulation of apoptosis for cancer therapy using BH3-mimetic drugs. *Nat. Rev. Cancer* **22**, 45–64 (2022).
43. A. W. Roberts, M. S. Davids, J. M. Pagel, B. S. Kahl, S. D. Puvvada, J. F. Gerecitano, T. J. Kipps, M. A. Anderson, J. R. Brown, L. Gressick, S. Wong, M. Dunbar, M. Zhu, M. B. Desai, E. Cerri, S. Heitner Enschede, R. A. Humerickhouse, W. G. Wierda, J. F. Seymour, Targeting BCL2 with venetoclax in relapsed chronic lymphocytic leukemia. *N. Engl. J. Med.* **374**, 311–322 (2016).
44. T. L. Deckwerth, J. L. Elliott, C. M. Knudson, E. M. Johnson Jr., W. D. Snider, S. J. Korsmeyer, BAX is required for neuronal death after trophic factor deprivation and during development. *Neuron* **17**, 401–411 (1996).
45. F. Edlich, S. Banerjee, M. Suzuki, M. M. Cleland, D. Arnoult, C. Wang, A. Neutzner, N. Tjandra, R. J. Youle, Bcl-x_L retrotranslocates Bax from the mitochondria into the cytosol. *Cell* **145**, 104–116 (2011).
46. B. Schellenberg, P. Wang, J. A. Keeble, R. Rodriguez-Enriquez, S. Walker, T. W. Owens, F. Foster, J. Tanianis-Hughes, K. Brennan, C. H. Streuli, A. P. Gilmore, Bax exists in a dynamic equilibrium between the cytosol and mitochondria to control apoptotic priming. *Mol. Cell* **49**, 959–971 (2013).
47. P. E. Czabotar, G. Lessene, A. Strasser, J. M. Adams, Control of apoptosis by the BCL-2 protein family: Implications for physiology and therapy. *Nat. Rev. Mol. Cell Biol.* **15**, 49–63 (2014).
48. A. Ashkenazi, W. J. Fairbrother, J. D. Leverson, A. J. Souers, From basic apoptosis discoveries to advanced selective BCL-2 family inhibitors. *Nat. Rev. Drug Discov.* **16**, 273–284 (2017).
49. G. Dewson, T. Kratina, H. W. Sim, H. Puthalakath, J. M. Adams, P. M. Colman, R. M. Kluck, To trigger apoptosis, Bak exposes its BH3 domain and homodimerizes via BH3:Groove interactions. *Mol. Cell* **30**, 369–380 (2008).
50. G. J. Griffiths, L. Dubrez, C. P. Morgan, N. A. Jones, J. Whitehouse, B. M. Corfe, C. Dive, J. A. Hickman, Cell damage-induced conformational changes of the pro-apoptotic protein Bak in vivo precede the onset of apoptosis. *J. Cell Biol.* **144**, 903–914 (1999).
51. J. Schredelseker, A. Paz, C. J. López, C. Altenbach, C. S. Leung, M. K. Drexler, J. N. Chen, W. L. Hubbell, J. Abramson, High resolution structure and double electron-electron resonance of the zebrafish voltage-dependent anion channel 2 reveal an oligomeric population. *J. Biol. Chem.* **289**, 12566–12577 (2014).
52. J. Jumper, R. Evans, A. Pritzel, T. Green, M. Figurnov, O. Ronneberger, K. Tunyasuvunakool, R. Bates, A. Žídek, A. Potapenko, A. Bridgland, C. Meyer, S. A. A. Kohl, A. J. Ballard, A. Cowie, B. Romera-Paredes, S. Nikolov, R. Jain, J. Adler, T. Back, S. Petersen, D. Reiman, E. Clancy, M. Zielinski, M. Steinegger, M. Pacholska, T. Berghammer, S. Bodenstein, D. Silver, O. Vinyals, A. W. Senior, K. Kavukcuoglu, P. Kohli, D. Hassabis, Highly accurate protein structure prediction with AlphaFold. *Nature* **596**, 583–589 (2021).
53. M. Varadi, D. Bertoni, P. Magana, U. Paramval, I. Pidruchna, M. Radhakrishnan, M. Tsenkov, S. Nair, M. Mirdita, J. Yeo, O. Kovalevskiy, K. Tunyasuvunakool, A. Laydon, A. Žídek, H. Tomlinson, D. Hariharan, J. Abrahamson, T. Green, J. Jumper, E. Birney, M. Steinegger, D. Hassabis, S. Velankar, AlphaFold protein structure database in 2024: Providing structure coverage for over 214 million protein sequences. *Nucleic Acids Res.* **52**, D368–D375 (2024).
54. X. Robert, P. Gouet, Deciphering key features in protein structures with the new ENDscript server. *Nucleic Acids Res.* **42**, W320–W324 (2014).

Acknowledgments: We thank A. Roberts for discussion and suggestions. We acknowledge Compounds Australia (www.compoundsaustralia.com) for provision of specialized compound management and logistics research services to the project. **Funding:** This work was supported by operational infrastructure grants through the Australian Government Independent Research Institute Infrastructure Support Scheme (9000587) and the Victorian State Government Operational Infrastructure Support, Australia. This work was also supported by the following: National Health and Medical Research Council, Australia 1043149 (D.C.S.H.); National Health and Medical Research Council, Australia 1156024 (to D.C.S.H.); National Health and Medical Research Council, Australia 2016894 (to R.W.B.); National Health and Medical Research Council, Australia 2009062 (to P.E.C.); National Health and Medical Research Council, Australia 1117089 (to G.L.); National Health and Medical Research Council, Australia 2018071 (to A.H.W.); National Health and Medical Research Council, Australia 2004446 (to G.D.); National Health and Medical Research Council, Australia 1158137 (to M.F.v.D.); National Health and Medical Research Council, Australia 1158137 (to P.E.C.); National Health and Medical Research Council, Australia 1158137 (to G.L.); Perpetual Impact Grant (to G.L.); Perpetual Impact Grant (to M.F.v.D.); Bodhi Education Fund (to G.D.); and Victorian Cancer Agency MCRF Fellowship 19011 (to D.M.M.). **Author contributions:** Conceptualization: K.Li., M.F.v.D., G.D., G.L., B.T.K., P.E.C., A.H.W., D.C.S.H., R.W.B., and Y.Q.Y. Methodology: Y.Q.Y., K.Li., M.F.v.D., D.M.M., Y.K., B.T.K., D.C.S.H., and G.L. Investigation: K.Li., Y.Q.Y., F.S., A.G., M.J., T.E.L., M.D.S., M.-X.L., J.-n.G., Z.Y., D.M.M., Y.K., and K.Lo. Validation: D.M.M., K.Li., and G.L. Visualization: K.Li., D.C.S.H., and G.L. Data curation: K.Li. Formal analysis: K.Lo., D.M.M., K.Li., G.L., and M.J. Project administration: G.D., M.F.v.D., G.L., B.T.K., K.Li., and D.C.S.H. Supervision: G.D., M.F.v.D., G.L., B.T.K., and D.C.S.H. Resources: B.T.K., K.Li., J.-n.G., D.C.S.H., G.L., G.D., and M.D.S. Funding acquisition: D.C.S.H., G.L., and G.D. Writing (original draft): K.Li., D.M.M., Y.K., K.Lo., G.D., M.F.v.D., G.L., and D.C.S.H. Writing (review and editing): P.E.C., D.C.S.H., G.D., M.F.v.D., G.L., K.Li., and B.T.K. **Competing interests:** G.D., P.E.C., R.B., D.C.S.H., M.F.v.D., G.L., Y.Q.Y., D.M.M., F.S., Y.K., A.G., R.W.B., P.E.C., K.Lo., and A.H.W. are employees of the Walter and Eliza Hall Institute of Medical Research that receives milestone payments related to sales of venetoclax. A.H.W. provides medical advice and receives honoraria and research funding to the institution from AbbVie. The other authors declare that they have no competing interests. **Data and materials availability:** All data needed to evaluate the conclusions in the paper are present in the paper and/or the Supplementary Materials.

Submitted 21 July 2024
Accepted 30 January 2025
Published 5 March 2025
10.1126/sciadv.adr8146